

Observation of the $X(2370)$ in $J/\psi \rightarrow \gamma K_S^0 K_S^0 \pi^0$ and $J/\psi \rightarrow \gamma \pi^0 \pi^0 \eta$

M. Ablikim¹, M. N. Achasov^{4,c}, P. Adlarson⁸³, X. C. Ai⁸⁹, C. S. Akondi^{31A,31B}, R. Aliberti³⁹, A. Amoroso^{82A,82C}, Q. An^{78,65,†}, Y. H. An⁸⁹, M. S. Anderson³⁹, Y. Bai⁶³, O. Bakina⁴⁰, H. R. Bao⁷¹, X. L. Bao⁵⁰, M. Barbaggio^{82C}, V. Batzokskaya^{1,49}, K. Begzsuren³⁵, N. Berger³⁹, M. Berlowski⁴⁹, M. B. Bertani^{30A}, D. Bettoni^{31A}, F. Bianchi^{82A,82C}, E. Bianco^{82A,82C}, A. Bortone^{82A,82C}, I. Boyko⁴⁰, R. A. Briere⁵, A. Brueggemann⁷⁵, D. Cabibbi^{69A}, H. Cai⁸⁴, M. H. Cai^{42,k,l}, X. Cai^{1,65}, A. Calcaterra^{30A}, G. F. Cao^{1,71}, N. Cao^{1,71}, S. A. Cetin^{69A}, X. Y. Chal^{51,h}, J. F. Chang^{1,65}, T. T. Chang⁴⁸, G. R. Che⁴⁸, Y. Z. Che^{1,65,71}, C. H. Chen¹⁰, Chao Chen¹, G. Chen¹, H. S. Chen^{1,71}, H. Y. Chen²⁰, M. L. Chen^{1,65,71}, S. J. Chen⁴⁷, S. M. Chen⁶⁸, T. Chen^{1,71}, W. Chen⁵⁰, X. R. Chen^{34,71}, X. T. Chen^{1,71}, X. Y. Chen^{12,g}, Y. B. Chen^{1,65}, Y. Q. Chen¹⁶, Z. K. Chen⁶⁶, J. Cheng⁵⁰, L. N. Cheng⁴⁸, S. K. Choi¹¹, X. Chu^{12,g}, G. Cibinetto^{31A}, F. Cossio^{82C}, J. Cottee-Meldrum⁷⁰, H. L. Dai^{1,65}, J. P. Dai⁸⁷, X. C. Dai⁶⁸, A. Dbeyssi¹⁹, R. E. de Boer³, D. Dedovich⁴⁰, C. Q. Deng⁸⁰, Z. Y. Deng¹, A. Denig³⁹, I. Denisenko⁴⁰, M. Destefanis^{82A,82C}, F. De Mori^{82A,82C}, E. Di Fiore^{31A,31B}, X. X. Ding^{51,h}, Y. Ding⁴⁴, Y. X. Ding³², J. Dong^{1,65}, L. Y. Dong^{1,71}, M. Y. Dong^{1,65,71}, X. Dong⁸⁴, Z. J. Dong⁶⁶, M. C. Du¹, S. X. Du⁸⁹, Shaoyu Du^{12,g}, X. L. Du^{12,g}, Y. Q. Du⁸⁴, Y. Y. Duan⁶¹, Z. H. Duan⁴⁷, P. Egorov^{40,a}, G. F. Fan⁴⁷, J. J. Fan²⁰, Y. H. Fan⁵⁰, J. Fang^{1,65}, Jin Fang⁶⁶, S. S. Fang^{1,71}, W. X. Fang¹, Y. Q. Fang^{1,65,†}, L. Fava^{82B,82C}, F. Feldbauer³, G. Felici^{30A}, C. Q. Feng^{78,65}, J. H. Feng¹⁶, Q. X. Feng^{42,k,l}, Y. T. Feng^{78,65}, M. Fritsch³, C. D. Fu¹, J. L. Fu⁷¹, Y. W. Fu^{1,71}, H. Gao⁷¹, Xu Gao³⁸, Y. Gao^{78,65}, Y. N. Gao^{51,h}, Y. Y. Gao³², Yunong Gao²⁰, Z. Gao⁴⁸, S. Garbolino^{82C}, I. Garzia^{31A,31B}, L. Ge⁶³, P. T. Ge²⁰, Z. W. Ge⁴⁷, C. Geng⁶⁶, A. Gilman⁷⁶, K. Goetzen¹³, J. Gollub³, J. B. Gong^{1,71}, J. D. Gong³⁸, L. Gong⁴⁴, W. X. Gong^{1,65}, W. Grad³⁹, M. Greco^{82A,82C}, M. D. Gu⁵⁶, M. H. Gu^{1,65}, C. Y. Guan^{1,71}, A. Q. Guo³⁴, H. Guo⁵⁵, J. N. Guo^{12,g}, L. B. Guo⁴⁶, M. J. Guo⁵⁵, R. P. Guo⁵⁴, X. Guo⁵⁵, Y. P. Guo^{12,g}, Z. Guo^{78,65}, A. Guskov^{40,a}, J. Gutierrez²⁹, M. J. Han^{78,65}, T. T. Han¹, X. Han^{78,65}, F. Hanisch³, K. D. Hao^{78,65}, X. Q. Hao²⁰, F. A. Harris⁷², C. Z. He^{51,h}, K. K. He^{17,47}, K. L. He^{1,71}, F. H. Heinsius³, C. H. Heinz³⁹, Y. K. Heng^{1,65,71}, C. Herold⁶⁷, P. C. Hong³⁸, G. Y. Hou^{1,71}, X. T. Hou^{1,71}, Y. R. Hou⁷¹, Z. L. Hou¹, H. M. Hu^{1,71}, J. F. Hu^{62,j}, Q. P. Hu^{78,65}, S. L. Hu^{12,g}, T. Hu^{1,65,71}, Y. Hu¹, Y. X. Hu⁸⁴, Z. M. Hu⁶⁶, G. S. Huang^{78,65}, K. X. Huang⁶⁶, L. Q. Huang^{34,71}, P. Huang⁴⁷, X. T. Huang⁵⁵, Y. P. Huang¹, Y. S. Huang⁶⁶, T. Hussain⁸¹, N. Hüsken³⁹, N. in der Wiesche⁷⁵, J. Jackson²⁹, Q. Ji¹, Q. P. Ji²⁰, W. Ji^{1,71}, X. B. Ji^{1,71}, X. L. Ji^{1,65}, Y. Y. Ji¹, L. K. Jia⁷¹, X. Q. Jia⁵⁵, D. Jiang^{1,71}, S. J. Jiang¹⁰, X. S. Jiang^{1,65,71}, Y. Jiang⁷¹, J. B. Jiao⁵⁵, J. K. Jiao³⁸, Z. Jiao²⁵, L. C. L. Jin¹, S. Jin⁴⁷, Y. Jin⁷³, M. Q. Jing⁵⁶, X. M. Jing⁷¹, T. Johansson⁸³, S. Kabana³⁶, X. L. Kang¹⁰, X. S. Kang⁴⁴, B. C. Ke⁸⁹, V. Khachatryan²⁹, A. Khokkaz⁷⁵, O. B. Kolcu^{69A}, B. Kopf³, L. Kröger⁷⁵, L. Krümmel³, Y. Y. Kuang⁸⁰, X. Kui^{1,71}, N. Kumar²⁸, A. Kupsc^{49,83}, W. Kühn⁴¹, Q. Lan⁸⁰, W. N. Lan²⁰, T. T. Lei^{78,65}, M. Lellmann³⁹, T. Lenz³⁹, C. Li⁵², C. H. Li⁴⁶, C. K. Li⁴⁸, Chunkai Li²¹, Cong Li⁴⁸, D. M. Li⁸⁹, F. Li^{1,65}, G. Li¹, H. B. Li^{1,71}, H. J. Li²⁰, H. L. Li⁸⁹, H. N. Li^{62,j}, H. P. Li⁴⁸, Hui Li⁴⁸, J. N. Li³², J. S. Li⁶⁶, J. W. Li⁵⁵, K. Li¹, K. L. Li^{42,k,l}, L. J. Li^{1,71}, L. K. Li²⁶, Lei Li⁵³, M. H. Li⁴⁸, M. R. Li^{1,71}, M. T. Li⁵⁵, P. L. Li⁷¹, P. R. Li^{42,k,l}, Q. M. Li^{1,71}, Q. X. Li⁵⁵, R. Li^{18,34}, S. Li⁸⁹, S. X. Li⁸⁹, S. Y. Li⁸⁹, Shanshan Li^{27,i}, T. Li⁵⁵, T. Y. Li⁴⁸, W. D. Li^{1,71}, W. G. Li^{1,†}, X. Li^{1,71}, X. H. Li^{78,65}, X. K. Li^{51,h}, X. L. Li⁵⁵, X. Y. Li^{78,65}, X. Z. Li⁶⁶, Y. Li²⁰, Y. H. Li⁴⁸, Y. B. Li⁸⁵, Y. C. Li⁶⁶, Y. G. Li⁷¹, Y. P. Li³⁸, Z. H. Li⁴², Z. J. Li⁶⁶, Z. L. Li⁸⁹, Z. X. Li⁴⁸, Z. Y. Li⁸⁷, C. Liang⁴⁷, H. Liang^{78,65}, Y. F. Liang⁶⁰, Y. T. Liang^{34,71}, Z. Z. Liang⁶⁶, G. R. Liao¹⁴, L. B. Liao⁶⁶, M. H. Liao⁶⁶, Y. P. Liao^{1,71}, J. Libby²⁸, A. Limphirat⁶⁷, C. C. Lin⁶¹, C. X. Lin³⁴, D. X. Lin^{34,71}, T. Lin¹, B. J. Liu¹, B. X. Liu⁸⁴, C. Liu³⁸, C. X. Liu¹, F. Liu¹, F. H. Liu⁵⁹, Feng Liu⁶, G. M. Liu^{62,j}, H. Liu^{42,k,l}, H. B. Liu¹⁵, H. M. Liu^{1,71}, Huihui Liu²², J. B. Liu^{78,65}, J. J. Liu²¹, K. Liu^{42,k,l}, K. Y. Liu⁴⁴, Ke Liu²³, Kun Liu⁸⁰, L. Liu⁴², L. C. Liu⁴⁸, Lu Liu⁴⁸, M. H. Liu³⁸, P. L. Liu⁵⁵, Q. Liu⁷¹, S. B. Liu^{78,65}, T. Liu¹, W. M. Liu^{78,65}, W. T. Liu⁴³, X. Liu^{42,k,l}, X. K. Liu⁸⁹, Z. A. Liu^{1,65,71}, Z. D. Liu⁸⁵, Z. L. Liu⁸⁰, X. T. Liu²¹, X. Y. Liu⁸⁴, Y. Liu^{42,k,l}, Y. B. Liu⁴⁸, Yi Liu⁸⁹, Z. A. Liu^{1,65,71}, Z. D. Liu⁸⁵, Z. L. Liu⁸⁰, Z. Q. Liu⁵⁵, Z. X. Liu¹, Z. Y. Liu⁴², X. C. Lou^{1,65,71}, H. J. Lu²⁵, J. G. Lu^{1,65}, X. L. Lu¹⁶, Y. Lu⁷, Y. H. Lu^{1,71}, Y. P. Lu^{1,65}, Z. H. Lu^{1,71}, C. L. Luo⁴⁶, J. R. Luo⁶⁶, J. S. Luo^{1,71}, M. X. Luo⁸⁸, T. Luo^{12,g}, X. L. Luo^{1,65}, Z. Y. Lv²³, X. R. Lyu^{71,o}, Y. F. Lyu⁴⁸, Y. H. Lyu⁸⁹, F. C. Ma⁴⁴, H. L. Ma¹, Heng Ma^{27,i}, J. L. Ma^{1,71}, L. L. Ma⁵⁵, L. R. Ma⁷³, Q. M. Ma¹, R. Q. Ma^{1,71}, R. Y. Ma²⁰, T. Ma^{78,65}, X. T. Ma^{1,71}, X. Y. Ma^{1,65}, F. E. Maas¹⁹, I. MacKay⁷⁶, M. Maggiora^{82A,82C}, S. Maity³⁴, S. Malde⁷⁶, L. M. Mansur³⁹, Y. J. Mao^{51,h}, Z. P. Mao¹, S. Marcello^{82A,82C}, A. Marshall⁷⁰, F. M. Melendi^{31A,31B}, Y. H. Meng⁷¹, Z. X. Meng⁷³, G. Mezzadri^{31A}, H. Miao^{1,71}, T. J. Min⁴⁷, R. E. Mitchell²⁹, X. H. Mo^{1,65,71}, B. Moses²⁹, N. Yu. Muchnoi^{4,c}, J. Muskalla³⁹, Y. Nefedov⁴⁰, F. Nerling^{19,e}, H. Neuwirth⁷⁵, Z. Ning^{1,65}, S. Nisar³³, Q. L. Niu^{42,k,l}, W. D. Niu^{12,g}, Y. Niu⁵⁵, C. Normand⁷⁰, S. L. Olsen^{11,71}, Q. Ouyang^{1,65,71}, I. V. Ovtin⁴, S. Pacetti^{30B,30C}, Y. Pan⁶³, C. Y. Pang¹⁴, A. Pathak¹¹, Y. P. Pei^{78,65}, M. Pelizaeus³, G. L. Peng^{78,65}, H. P. Peng^{78,65}, X. J. Peng^{42,k,l}, Y. Y. Peng^{42,k,l}, K. Peters^{13,e}, K. Petridis⁷⁰, J. L. Ping⁴⁶, R. G. Ping^{1,71}, S. Plura³⁹, V. Prasad³⁸, L. Pöpping³, F. Z. Qi¹, H. R. Qi⁶⁸, S. Qian^{1,65}, W. B. Qian⁷¹, C. F. Qiao⁷¹, J. H. Qiao²⁰, J. J. Qin⁸⁰, J. L. Qin⁶¹, L. Q. Qin¹⁴, L. Y. Qin^{78,65}, P. B. Qin⁸⁰, X. P. Qin⁴³, X. S. Qin⁵⁵, Z. H. Qin^{1,65}, J. F. Qiu¹, Z. H. Qu⁸⁰, J. Rademacker⁷⁰, K. Ravindran⁷⁴, C. F. Redmer³⁹, A. Rivetti^{82C}, M. Rolo^{82C}, G. Rong^{1,71}, S. S. Rong^{1,71}, F. Rosini^{30B,30C}, Ch. Rosner¹⁹, M. Q. Ruan^{1,65}, W. R. Ruangyoo⁶⁷, N. Salone⁷⁹, A. Sarantsev^{40,d}, Y. Schelhaas³⁹, M. Schernau³⁶, K. Schoenning⁸³,

M. Scodeggio^{31A} , W. Shan²⁶ , X. Y. Shan^{78,65} , Z. J. Shang^{42,k,l} , J. F. Shangguan¹⁷ , L. G. Shao^{1,71} ,
M. Shao^{78,65} , C. P. Shen^{12,g} , H. F. Shen^{1,9} , W. H. Shen⁷¹ , X. Y. Shen^{1,71} , B. A. Shi⁷¹ , Ch. Y. Shi^{87,b} ,
H. Shi^{78,65} , J. L. Shi^{8,p} , J. Y. Shi¹ , M. H. Shi⁸⁹ , S. Shi⁸⁰ , S. Y. Shi⁸⁰ , X. Shi^{1,65} , H. L. Song^{78,65} ,
J. J. Song²⁰ , M. H. Song⁴² , T. Z. Song⁶⁶ , W. M. Song³⁸ , Y. X. Song^{51,h,m} , Zirong Song^{27,i} , S. Sosio^{82A,82C} ,
S. Spataro^{82A,82C} , S. Stansilau⁷⁶ , F. Stieler³⁹ , M. Stolte³ , S. S. Su⁴⁴ , G. B. Sun⁸⁴ , G. X. Sun¹ , H. Sun⁷¹ ,
H. K. Sun¹ , J. F. Sun²⁰ , K. Sun⁶⁸ , L. Sun⁸⁴ , R. Sun⁷⁸ , S. S. Sun^{1,71} , T. Sun^{57,f} , W. Y. Sun⁵⁶ ,
Y. C. Sun⁸⁴ , Y. H. Sun³² , Y. J. Sun^{78,65} , Y. Z. Sun¹ , Z. Q. Sun^{1,71} , Z. T. Sun⁵⁵ , H. Tabaharizato¹ ,
N. T. Tagsinsit⁶⁷ , C. J. Tang⁶⁰ , G. Y. Tang¹ , J. Tang⁶⁶ , J. J. Tang^{78,65} , L. F. Tang⁴³ , Y. A. Tang⁸⁴ ,
Z. H. Tang^{1,71} , L. Y. Tao⁸⁰ , M. Tat⁷⁶ , J. X. Teng^{78,65} , J. Y. Tian^{78,65} , W. H. Tian⁶⁶ , Y. Tian³⁴ ,
Z. F. Tian⁸⁴ , K. Yu. Todyshev⁴ , I. Uman^{69B} , E. van der Smagt³ , B. Wang⁶⁶ , Bin Wang¹ , Bo Wang^{78,65} ,
C. Wang^{42,k,l} , Chao Wang²⁰ , Cong Wang²³ , D. Y. Wang^{51,h} , F. K. Wang⁶⁶ , H. J. Wang^{42,k,l} , H. R. Wang⁸⁶ ,
J. Wang¹⁰ , J. J. Wang⁸⁴ , J. P. Wang³⁷ , K. Wang^{1,65} , L. L. Wang¹ , L. W. Wang³⁸ , M. Wang⁵⁵ ,
Mi Wang^{78,65} , N. Y. Wang⁷¹ , P. Wang²¹ , S. Wang^{42,k,l} , Shun Wang⁶⁴ , T. Wang^{12,g} , W. Wang⁶⁶ ,
W. P. Wang³⁹ , X. F. Wang^{42,k,l} , X. L. Wang^{12,g} , X. N. Wang^{1,71} , Xin Wang^{27,i} , Y. Wang¹ , Y. D. Wang⁵⁰ ,
Y. F. Wang^{1,9,71} , Y. H. Wang^{42,k,l} , Y. J. Wang^{78,65} , Y. L. Wang²⁰ , Y. N. Wang⁵⁰ , Yanping Wang⁸⁴ ,
Yaqian Wang¹⁸ , Yi Wang⁶⁸ , Yuan Wang^{18,34} , Z. Wang^{1,65} , Z. L. Wang² , Z. Q. Wang^{12,g} , Z. Y. Wang^{1,71} ,
Zhi Wang⁴⁸ , Ziyi Wang⁷¹ , D. Wei⁴⁸ , D. H. Wei¹⁴ , D. J. Wei⁷³ , H. R. Wei⁴⁸ , F. Weidner⁷⁵ , H. R. Wen³⁴ ,
S. P. Wen¹ , U. Wiedner³ , G. Wilkinson⁷⁶ , J. F. Wu^{1,9} , L. H. Wu¹ , L. J. Wu²⁰ , Lianjie Wu²⁰ , S. G. Wu^{1,71} ,
S. M. Wu⁷¹ , X. W. Wu⁸⁰ , Z. Wu^{1,65} , H. L. Xia^{78,65} , L. Xia^{78,65} , B. H. Xiang^{1,71} , D. Xiao^{42,k,l} ,
G. Y. Xiao⁴⁷ , H. Xiao⁸⁰ , Y. L. Xiao^{12,g} , Z. J. Xiao⁴⁶ , C. Xie⁴⁷ , K. J. Xie^{1,71} , Y. Xie⁵⁵ , Y. G. Xie^{1,65} ,
Y. H. Xie⁶ , Z. P. Xie^{78,65} , T. Y. Xing^{1,71} , D. B. Xiong¹ , G. F. Xu¹ , H. Y. Xu² , Q. J. Xu¹⁷ , Q. N. Xu³² ,
T. D. Xu⁸⁰ , X. P. Xu⁶¹ , Y. Xu^{12,g} , Y. C. Xu⁸⁶ , Z. S. Xu⁷¹ , F. Yan²⁴ , L. Yan^{12,g} , W. B. Yan^{78,65} ,
W. C. Yan⁸⁹ , W. H. Yan⁶ , W. P. Yan²⁰ , X. Q. Yan^{12,g} , Y. Y. Yan⁶⁷ , H. J. Yang^{57,f} , H. L. Yang³⁸ ,
H. X. Yang¹ , J. H. Yang⁴⁷ , R. J. Yang²⁰ , X. Y. Yang⁷³ , Y. Yang^{12,g} , Y. G. Yang⁵⁶ , Y. H. Yang⁴⁸ ,
Y. M. Yang⁸⁹ , Y. Q. Yang¹⁰ , Y. Z. Yang²⁰ , Youhua Yang⁴⁷ , Z. Y. Yang⁸⁰ , W. J. Yao⁶ , Z. P. Yao⁵⁵ ,
M. Ye^{1,65} , M. H. Ye^{9,i} , Z. J. Ye^{62,j} , K. Yi⁴⁶ , Junhao Yin⁴⁸ , Q. Q. Yin⁴⁸ , Z. Y. You⁶⁶ , B. X. Yu^{1,65,71} ,
C. X. Yu⁴⁸ , G. Yu¹³ , J. S. Yu^{27,i} , L. W. Yu^{12,g} , T. Yu⁸⁰ , X. D. Yu^{51,h} , Y. C. Yu⁸⁹ , Yongchao Yu⁴² ,
C. Z. Yuan^{1,71} , H. Yuan^{1,71} , J. Yuan³⁸ , Jie Yuan⁵⁰ , L. Yuan² , M. K. Yuan^{12,g} , S. H. Yuan⁸⁰ , Y. Yuan^{1,71} ,
C. X. Yue⁴³ , Ying Yue²⁰ , A. A. Zafar⁸¹ , F. R. Zeng⁵⁵ , S. H. Zeng⁷⁰ , X. Zeng^{12,g} , Y. J. Zeng^{1,71} ,
Yujie Zeng⁶⁶ , Y. C. Zhai⁵⁵ , Y. H. Zhan⁶⁶ , B. L. Zhang^{1,71} , B. X. Zhang^{1,i} , D. H. Zhang⁴⁸ , G. Y. Zhang²⁰ ,
Gengyuan Zhang^{1,71} , H. Zhang^{78,65} , H. C. Zhang^{1,65,71} , H. H. Zhang⁶⁶ , H. L. Zhang⁴⁸ , H. Q. Zhang^{1,65,71} ,
H. R. Zhang^{78,65} , H. Y. Zhang^{1,65} , Han Zhang⁸⁹ , J. Zhang⁶⁶ , J. J. Zhang⁵⁸ , J. L. Zhang²¹ , J. Q. Zhang⁴⁶ ,
J. S. Zhang^{12,g} , J. W. Zhang^{1,65,71} , J. X. Zhang^{42,k,l} , J. Y. Zhang¹ , J. Z. Zhang^{1,71} , Jianyu Zhang⁴⁹ ,
Jin Zhang⁵³ , Jiyan Zhang^{12,g} , L. M. Zhang⁶⁸ , Lei Zhang⁴⁷ , N. Zhang³⁸ , P. Zhang^{1,9} , Q. Zhang²⁰ ,
Q. Y. Zhang³⁸ , Q. Z. Zhang⁷¹ , R. Y. Zhang^{42,k,l} , S. H. Zhang^{1,71} , S. N. Zhang⁷⁶ , Shulei Zhang^{27,i} ,
X. M. Zhang¹ , X. Y. Zhang⁵⁵ , Y. T. Zhang⁸⁹ , Y. H. Zhang^{1,65} , Y. P. Zhang^{78,65} , Yao Zhang¹ , Yu Zhang⁸⁰ ,
Yu Zhang⁶⁶ , Z. Zhang³⁴ , Z. D. Zhang¹ , Z. H. Zhang¹ , Z. L. Zhang³⁸ , Z. X. Zhang²⁰ , Z. Y. Zhang⁸⁴ ,
Zh. Zh. Zhang²⁰ , Zhilong Zhang⁶¹ , Ziyang Zhang⁵⁰ , Ziyu Zhang⁴⁸ , G. Zhao¹ , J.-P. Zhao⁷¹ , J. Y. Zhao^{1,71} ,
J. Z. Zhao^{1,65} , L. Zhao¹ , Lei Zhao^{78,65} , M. G. Zhao⁴⁸ , R. P. Zhao⁷¹ , S. J. Zhao⁸⁹ , Y. B. Zhao^{1,65} ,
Y. L. Zhao⁶¹ , Y. P. Zhao

- ¹⁷ Hangzhou Normal University, Hangzhou 310036, People's Republic of China
- ¹⁸ Hebei University, Baoding 071002, People's Republic of China
- ¹⁹ Helmholtz Institute Mainz, Staudinger Weg 18, D-55099 Mainz, Germany
- ²⁰ Henan Normal University, Xinxiang 453007, People's Republic of China
- ²¹ Henan University, Kaifeng 475004, People's Republic of China
- ²² Henan University of Science and Technology, Luoyang 471003, People's Republic of China
- ²³ Henan University of Technology, Zhengzhou 450001, People's Republic of China
- ²⁴ Hengyang Normal University, Hengyang 421002, People's Republic of China
- ²⁵ Huangshan College, Huangshan 245000, People's Republic of China
- ²⁶ Hunan Normal University, Changsha 410081, People's Republic of China
- ²⁷ Hunan University, Changsha 410082, People's Republic of China
- ²⁸ Indian Institute of Technology Madras, Chennai 600036, India
- ²⁹ Indiana University, Bloomington, Indiana 47405, USA
- ³⁰ INFN Laboratori Nazionali di Frascati, (A)INFN Laboratori Nazionali di Frascati, I-00044, Frascati, Italy; (B)INFN Sezione di Perugia, I-06100, Perugia, Italy; (C)University of Perugia, I-06100, Perugia, Italy
- ³¹ INFN Sezione di Ferrara, (A)INFN Sezione di Ferrara, I-44122, Ferrara, Italy; (B)University of Ferrara, I-44122, Ferrara, Italy
- ³² Inner Mongolia University, Hohhot 010021, People's Republic of China
- ³³ Institute of Business Administration, University Road, Karachi, 75270 Pakistan
- ³⁴ Institute of Modern Physics, Lanzhou 730000, People's Republic of China
- ³⁵ Institute of Physics and Technology, Mongolian Academy of Sciences, Peace Avenue 54B, Ulaanbaatar 13330, Mongolia
- ³⁶ Instituto de Alta Investigación, Universidad de Tarapacá, Casilla 7D, Arica 1000000, Chile
- ³⁷ Jiangsu Ocean University, Lianyungang 222005, People's Republic of China
- ³⁸ Jilin University, Changchun 130012, People's Republic of China
- ³⁹ Johannes Gutenberg University of Mainz, Johann-Joachim-Becher-Weg 45, D-55099 Mainz, Germany
- ⁴⁰ Joint Institute for Nuclear Research, 141980 Dubna, Moscow region, Russia
- ⁴¹ Justus-Liebig-Universität Giessen, II. Physikalisches Institut, Heinrich-Buff-Ring 16, D-35392 Giessen, Germany
- ⁴² Lanzhou University, Lanzhou 730000, People's Republic of China
- ⁴³ Liaoning Normal University, Dalian 116029, People's Republic of China
- ⁴⁴ Liaoning University, Shenyang 110036, People's Republic of China
- ⁴⁵ Longyan University, Longyan 364000, People's Republic of China
- ⁴⁶ Nanjing Normal University, Nanjing 210023, People's Republic of China
- ⁴⁷ Nanjing University, Nanjing 210093, People's Republic of China
- ⁴⁸ Nankai University, Tianjin 300071, People's Republic of China
- ⁴⁹ National Centre for Nuclear Research, Warsaw 02-093, Poland
- ⁵⁰ North China Electric Power University, Beijing 102206, People's Republic of China
- ⁵¹ Peking University, Beijing 100871, People's Republic of China
- ⁵² Qufu Normal University, Qufu 273165, People's Republic of China
- ⁵³ Renmin University of China, Beijing 100872, People's Republic of China
- ⁵⁴ Shandong Normal University, Jinan 250014, People's Republic of China
- ⁵⁵ Shandong University, Jinan 250100, People's Republic of China
- ⁵⁶ Shandong University of Technology, Zibo 255000, People's Republic of China
- ⁵⁷ Shanghai Jiao Tong University, Shanghai 200240, People's Republic of China
- ⁵⁸ Shanxi Normal University, Linfen 041004, People's Republic of China
- ⁵⁹ Shanxi University, Taiyuan 030006, People's Republic of China
- ⁶⁰ Sichuan University, Chengdu 610064, People's Republic of China
- ⁶¹ Soochow University, Suzhou 215006, People's Republic of China
- ⁶² South China Normal University, Guangzhou 510006, People's Republic of China
- ⁶³ Southeast University, Nanjing 211100, People's Republic of China
- ⁶⁴ Southwest University of Science and Technology, Mianyang 621010, People's Republic of China
- ⁶⁵ State Key Laboratory of Particle Detection and Electronics, Beijing 100049, Hefei 230026, People's Republic of China
- ⁶⁶ Sun Yat-Sen University, Guangzhou 510275, People's Republic of China
- ⁶⁷ Suranaree University of Technology, University Avenue 111, Nakhon Ratchasima 30000, Thailand
- ⁶⁸ Tsinghua University, Beijing 100084, People's Republic of China
- ⁶⁹ Turkish Accelerator Center Particle Factory Group, (A)Istinye University, 34010, Istanbul, Turkey; (B)Near East University, Nicosia, North Cyprus, 99138, Mersin 10, Turkey
- ⁷⁰ University of Bristol, H H Wills Physics Laboratory, Tyndall Avenue, Bristol, BS8 1TL, UK
- ⁷¹ University of Chinese Academy of Sciences, Beijing 100049, People's Republic of China
- ⁷² University of Hawaii, Honolulu, Hawaii 96822, USA
- ⁷³ University of Jinan, Jinan 250022, People's Republic of China
- ⁷⁴ University of La Serena, Av. Raúl Bitrán 1305, La Serena, Chile
- ⁷⁵ University of Muenster, Wilhelm-Klemm-Strasse 9, 48149 Muenster, Germany
- ⁷⁶ University of Oxford, Keble Road, Oxford OX13RH, United Kingdom
- ⁷⁷ University of Science and Technology Liaoning, Anshan 114051, People's Republic of China

⁷⁸ *University of Science and Technology of China, Hefei 230026, People's Republic of China*

⁷⁹ *University of Silesia in Katowice, Institute of Physics, 75 Pulkta Piechoty 1, 41-500 Chorzow, Poland*

⁸⁰ *University of South China, Hengyang 421001, People's Republic of China*

⁸¹ *University of the Punjab, Lahore-54590, Pakistan*

⁸² *University of Turin and INFN, (A)University of Turin, I-10125, Turin, Italy; (B)University of Eastern Piedmont, I-15121, Alessandria, Italy; (C)INFN, I-10125, Turin, Italy*

⁸³ *Uppsala University, Box 516, SE-75120 Uppsala, Sweden*

⁸⁴ *Wuhan University, Wuhan 430072, People's Republic of China*

⁸⁵ *Xi'an Jiaotong University, No.28 Xianning West Road, Xi'an, Shaanxi 710049, P.R. China*

⁸⁶ *Yantai University, Yantai 264005, People's Republic of China*

⁸⁷ *Yunnan University, Kunming 650500, People's Republic of China*

⁸⁸ *Zhejiang University, Hangzhou 310027, People's Republic of China*

⁸⁹ *Zhengzhou University, Zhengzhou 450001, People's Republic of China*

[†] *Deceased*

^a *Also at the Moscow Institute of Physics and Technology, Moscow 141700, Russia*

^b *Also at the Functional Electronics Laboratory, Tomsk State University, Tomsk, 634050, Russia*

^c *Also at the Novosibirsk State University, Novosibirsk, 630090, Russia*

^d *Also at the NRC "Kurchatov Institute", PNPI, 188300, Gatchina, Russia*

^e *Also at Goethe University Frankfurt, 60323 Frankfurt am Main, Germany*

^f *Also at Key Laboratory for Particle Physics, Astrophysics and Cosmology, Ministry of Education; Shanghai Key Laboratory for Particle Physics and Cosmology; Institute of Nuclear and Particle Physics, Shanghai 200240, People's Republic of China*

^g *Also at Key Laboratory of Nuclear Physics and Ion-beam Application (MOE) and Institute of Modern Physics, Fudan University, Shanghai 200443, People's Republic of China*

^h *Also at State Key Laboratory of Nuclear Physics and Technology, Peking University, Beijing 100871, People's Republic of China*

ⁱ *Also at School of Physics and Electronics, Hunan University, Changsha 410082, China*

^j *Also at Guangdong Provincial Key Laboratory of Nuclear Science, Institute of Quantum Matter, South China Normal University, Guangzhou 510006, China*

^k *Also at MOE Frontiers Science Center for Rare Isotopes, Lanzhou University, Lanzhou 730000, People's Republic of China*

^l *Also at Lanzhou Center for Theoretical Physics, Lanzhou University, Lanzhou 730000, People's Republic of China*

^m *Also at Ecole Polytechnique Federale de Lausanne (EPFL), CH-1015 Lausanne, Switzerland*

ⁿ *Also at Helmholtz Institute Mainz, Staudinger Weg 18, D-55099 Mainz, Germany*

^o *Also at Hangzhou Institute for Advanced Study, University of Chinese Academy of Sciences, Hangzhou 310024, China*

^p *Also at Applied Nuclear Technology in Geosciences Key Laboratory of Sichuan Province, Chengdu University of Technology, Chengdu 610059, People's Republic of China*

Based on $(10087 \pm 44) \times 10^6$ J/ψ events collected with the BESIII detector, the $J/\psi \rightarrow \gamma K_S^0 K_S^0 \pi^0$ and $J/\psi \rightarrow \gamma \pi^0 \pi^0 \eta$ processes are studied. The $X(2370)$ is observed in both the $K_S^0 K_S^0 \pi^0$ and $\pi^0 \pi^0 \eta$ invariant mass spectra, with statistical significances greater than 14σ and 20σ , respectively. Combining measurements from these processes with measurements from the previously reported $J/\psi \rightarrow \gamma K_S^0 K_S^0 \eta'$ process, the mass and width of the $X(2370)$ are determined to be 2359_{-14}^{+13} MeV/ c^2 and 170_{-29}^{+44} MeV, respectively. In addition, the decay $X(2370) \rightarrow a_0(980)^0 \pi^0$ with $a_0(980)^0 \rightarrow \pi^0 \eta$ is observed with a statistical significance exceeding 9σ . The similarities in decay modes between the $X(2370)$ and η_c are consistent with the features of a pseudoscalar glueball.

Quantum Chromodynamics (QCD), a non-Abelian SU(3) gauge theory, predicts the existence of glueballs, which are uniquely formed by self-interacting gluons—the gauge bosons of the strong interactions. The search for glueballs in experiments is crucial for testing and developing QCD. Predictions of the 0^{-+} glueball mass from different lattice QCD (LQCD) groups are in the range of 2.3-3.0 GeV/ c^2 [1–6]. However, while J/ψ radiative decays are considered to be an ideal place for glueball searches [7–9], no 0^{-+} glueball candidates were observed in J/ψ radiative decays in the mass range above 2.3 GeV/ c^2 until 2011.

In 2011, based on a sample of 0.2 billion J/ψ events col-

lected with the BESIII detector, the $X(2370)$ particle was first observed in the process $J/\psi \rightarrow \gamma \pi^+ \pi^- \eta'$ with a statistical significance greater than 6.4σ . Its mass and width were measured to be $2376.3 \pm 8.7(\text{stat})_{-4.3}^{+3.2}(\text{syst})$ MeV/ c^2 and $83 \pm 17(\text{stat})_{-6}^{+44}(\text{syst})$ MeV [10], respectively. The observation is particularly interesting because the measured mass is consistent with the range predicted by LQCD for the lightest pseudoscalar glueball. Moreover, J/ψ radiative decays are generally considered to be a favorable environment for the production of glueballs, and a pseudoscalar glueball is expected to decay into channels like $\pi^+ \pi^- \eta'$ [10]. In subsequent studies, with 1.3 billion J/ψ events, the $X(2370)$ was con-

firmed in the decays $J/\psi \rightarrow \gamma K^+ K^- \eta'$ and $J/\psi \rightarrow \gamma K_S^0 K_S^0 \eta'$ with a statistical significance of 8.3σ [11]. Furthermore, using 10 billion J/ψ events, the spin-parity quantum numbers of the $X(2370)$ were determined to be 0^{-+} with a significance greater than 9.8σ in the $J/\psi \rightarrow \gamma K_S^0 K_S^0 \eta'$ process [12]. Its mass and width were measured to be $2395 \pm 11(\text{stat})_{-94}^{+26}(\text{syst})$ MeV/ c^2 and $188_{-17}^{+18}(\text{stat})_{-33}^{+124}(\text{syst})$ MeV, respectively. The product branching fraction of $J/\psi \rightarrow \gamma X(2370) \rightarrow \gamma f_0(980) \eta' \rightarrow \gamma K_S^0 K_S^0 \eta'$ was measured to be $(1.31 \pm 0.22(\text{stat})_{-0.84}^{+2.85}(\text{syst})) \times 10^{-5}$. The measured mass of the pseudoscalar $X(2370)$ is within the range predicted by LQCD for the lightest pseudoscalar glueball [5, 6]. Besides the glueball interpretation, there were also other interpretations and phenomenological studies on the $X(2370)$ [13–17]. In order to understand the nature of the $X(2370)$, more decay modes should be searched for and studied using 10 billion J/ψ decays collected at BESIII.

For the properties of glueball decays, there are no predictions from theory, including from LQCD. The idea that there are qualitative similarities between glueball decays and decays of charmonium states, since both decays proceed predominantly via gluons, was first proposed in Ref. [18]. In this picture, the 0^{++} and 2^{++} glueballs decays should be similar to χ_{c0} and χ_{c2} decays, respectively [18]. By analogy, the decays of a 0^{-+} glueball are expected to resemble those of the η_c [19–21], as illustrated in Fig. 1.

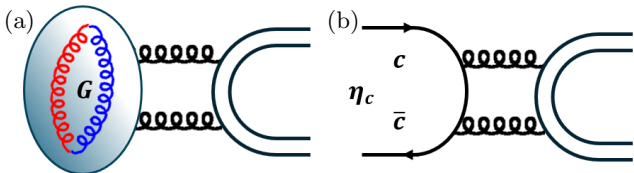


FIG. 1. (a) 0^{-+} glueball and (b) η_c decays.

The $KK\pi$ and $\pi\pi\eta$ modes are two typical decay processes of the η_c . In addition, the $\eta_c \rightarrow a_0(980)\pi$ decay has been observed, where the $a_0(980)$ dominantly decays into $\pi\eta$ [22]. Therefore, it is essential to search for corresponding decay modes of the $X(2370)$, such as $KK\pi$ and $\pi\pi\eta$, including the $a_0(980)\pi$ intermediate state, in order to investigate whether it can be interpreted as a pseudoscalar glueball. In this work, the $J/\psi \rightarrow \gamma K_S^0 K_S^0 \pi^0$ and $J/\psi \rightarrow \gamma \pi^0 \pi^0 \eta$ processes are studied. These channels benefit from very low background contributions since the processes $J/\psi \rightarrow \pi^0 K_S^0 K_S^0 \pi^0$ and $J/\psi \rightarrow \pi^0 \pi^0 \pi^0 \eta$ are forbidden by C -parity conservation and the exchange symmetry of identical particles ($K_S^0 K_S^0$ and $\pi^0 \pi^0$). This study is based on $(10087 \pm 44) \times 10^6$ J/ψ events [23] collected with the BESIII detector [24].

A detailed description of the design and performance of the BESIII detector can be found in Ref. [24]. Monte Carlo (MC) simulated data samples produced with a GEANT4-based [25] package, which includes the geometric description of the BESIII detector [26] and the detec-

tor response, are used to determine detection efficiencies and to estimate backgrounds. The simulation models the beam energy spread and initial state radiation in e^+e^- annihilations with the generator KKMC [27, 28]. The inclusive MC sample includes both the production of the J/ψ resonance and the continuum processes incorporated in KKMC [27, 28]. All particle decays are modelled with EVTGEN [29, 30] using branching fractions either taken from the Particle Data Group (PDG) [22], when available, or otherwise estimated with LUNDCHARM [31, 32]. Final state radiation from charged particles is incorporated using the PHOTOS package [33]. MC simulation samples of the processes $J/\psi \rightarrow \gamma K_S^0 K_S^0 \pi^0$ and $J/\psi \rightarrow \gamma \pi^0 \pi^0 \eta$, including the subsequent decays $K_S^0 \rightarrow \pi^+ \pi^-$, $\pi^0 \rightarrow \gamma\gamma$, and $\eta \rightarrow \gamma\gamma$, are generated uniformly in phase space (PHSP).

Charged tracks detected in the multi-layer drift chamber (MDC) are required to be within a polar angle (θ) range of $|\cos\theta| < 0.93$, where θ is defined with respect to the z -axis, which is the symmetry axis of the MDC. There is no requirement on the distance of closest approach to the interaction point for charged tracks since all charged tracks originate from K_S^0 decays. All charged tracks are assumed to be pions. To reconstruct K_S^0 candidates, the tracks of each $\pi^+ \pi^-$ pair are fitted to a secondary vertex. To suppress background events, all K_S^0 candidates are required to satisfy $|M_{\pi^+ \pi^-} - m_{K_S^0}| < 11$ MeV/ c^2 , where $m_{K_S^0}$ is the nominal mass of the K_S^0 from the PDG [22]. To further suppress background, the decay length of the K_S^0 candidate is required to be greater than twice the vertex resolution away from the interaction point. With these selections, the miscombination rate between pions from different K_S^0 is 0.2%. The reconstructed K_S^0 candidates are used as input for the subsequent kinematic fit.

Photon candidates are identified using isolated showers in the electromagnetic calorimeter (EMC). The deposited energy of each shower must be more than 25 MeV in the barrel region ($|\cos\theta| < 0.80$) and more than 50 MeV in the end cap region ($0.86 < |\cos\theta| < 0.92$). To exclude showers that originate from charged tracks, the opening angle between the shower position and charged tracks extrapolated to the EMC must be greater than 10 degrees. The EMC time of a shower is required to be within 700 ns after the e^+e^- annihilation (the time determined by charged tracks), or within 500 ns before and after the time of the highest-energy shower in the case of no charged tracks.

For the $J/\psi \rightarrow \gamma K_S^0 K_S^0 \pi^0$ process, each event candidate is required to have at least two K_S^0 candidates, at least three photons, and no additional charged tracks from the interaction point. A four-constraint (4C) kinematic fit under the $J/\psi \rightarrow \gamma\gamma\gamma K_S^0 K_S^0$ hypothesis is performed by enforcing energy-momentum conservation. If there are multiple $\gamma\gamma\gamma K_S^0 K_S^0$ combinations, the one with the smallest χ_{4C}^2 is chosen. The resulting χ_{4C}^2 is required to be less than 40. To reconstruct the π^0 candidate, a five-constraint (5C) kinematic fit is performed to further

constrain the invariant mass of the two photons to m_{π^0} , where m_{π^0} is the nominal mass of the π^0 [22]. Among the three $\gamma\gamma$ combinations, the one with the smallest χ_{5C}^2 is chosen as the π^0 candidate. The two photons from the π^0 candidate are required to satisfy $|M_{\gamma\gamma} - m_{\pi^0}| < 22$ MeV/ c^2 , with each photon having an energy greater than 100 MeV. To suppress miscombinations of the radiative photon (γ_{rad}) and the photons from the π^0 candidate (γ_{π^0}), events with $|M_{\gamma_{\text{rad}}\gamma_{\pi^0}} - m_{\pi^0}| < 22$ MeV/ c^2 are rejected. These photon-related requirements reduce the miscombination rate between the γ_{rad} and γ_{π^0} to 0.1%. Events with $|M_{\gamma_{\text{rad}}\gamma_{\pi^0}} - m_{\eta}| < 25$ MeV/ c^2 or $|M_{\gamma_{\text{rad}}\pi^0} - m_{\omega}| < 40$ MeV/ c^2 are rejected to suppress background containing an η or ω , where m_{η} and m_{ω} are the nominal masses of the η and ω [22], respectively. After applying the above selection criteria, a clear signature of the $X(2370)$ around 2.3 GeV/ c^2 , along with the η_c peak around 2.9 GeV/ c^2 , is observed in the $K_S^0 K_S^0 \pi^0$ invariant mass spectrum using the momenta obtained from the 5C kinematic fit, as shown in Fig. 2(a), Fig. 2(b), and Fig. 2(c). These two-dimensional distributions indicate several possible intermediate processes, for example, $a_0(980)^0 \pi^0$ and $K_0^*(1430) K_S^0 \rightarrow K_S^0 K_S^0 \pi^0$.

An inclusive MC sample of 10 billion J/ψ decays is used to study potential background contributions. After applying the above selection criteria to the inclusive MC sample, no peaking background is found in the $K_S^0 K_S^0 \pi^0$ invariant mass spectrum. The contributions of non- K_S^0 and non- π^0 background processes are found to be negligible in the data by fitting the corresponding $M_{\pi^+ \pi^-}$ and $M_{\gamma\gamma}$ distributions.

An unbinned maximum-likelihood fit is performed on the $K_S^0 K_S^0 \pi^0$ invariant mass spectrum between 1.95 and 2.75 GeV/ c^2 . The $X(2370)$ signal is described by an efficiency-corrected and PHSP-weighted Breit-Wigner (BW) function convoluted with a detector resolution function. A third-order polynomial function is used to describe the remaining processes. From the fit shown in Fig. 2(d), the mass and width of the $X(2370)$ are measured to be $2311 \pm 4(\text{stat})$ MeV/ c^2 and $177 \pm 20(\text{stat})$ MeV, respectively. The significance of the $X(2370)$ is greater than 14σ , which is determined from the changes in the log-likelihood value and degrees of freedom in fits with and without the $X(2370)$ signal hypothesis, and includes systematic variations.

For the $J/\psi \rightarrow \gamma\pi^0\pi^0\eta$ process, each event candidate is required to have no charged track and at least seven photons. To identify the photon pairs originating from π^0 decays, a one-constraint (1C) kinematic fit is performed by constraining the invariant mass of each photon pair to m_{π^0} . At least two pairs with $\chi_{1C}^2 < 10$ are required and are selected as π^0 candidates, which are then used as inputs to the subsequent kinematic fit. A six-constraint (6C) kinematic fit under the $J/\psi \rightarrow \gamma\gamma\pi^0\pi^0$ hypothesis is performed by enforcing energy-momentum conservation and constraining the invariant masses of two π^0 candidates to m_{π^0} . If there are multiple $\gamma\gamma\pi^0\pi^0$ combinations, the one with the smallest χ_{6C}^2 is chosen.

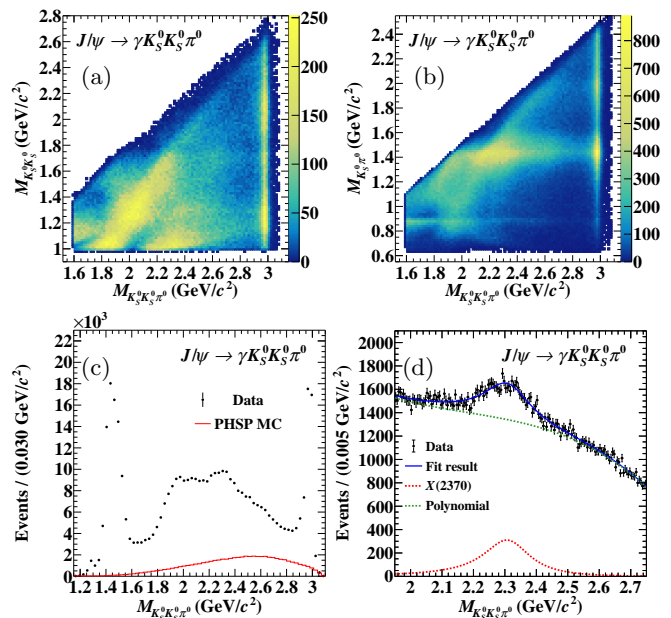


FIG. 2. The two-dimensional distributions of (a) $M_{K_S^0 K_S^0 \pi^0}$ versus $M_{K_S^0 K_S^0 \pi^0}$ and (b) $M_{K_S^0 \pi^0}$ versus $M_{K_S^0 K_S^0 \pi^0}$. (c) The $K_S^0 K_S^0 \pi^0$ invariant mass spectrum. The solid red histogram is from PHSP MC with arbitrary normalization. (d) The fit results within the range [1.95, 2.75] GeV/ c^2 . The dashed red line is the $X(2370)$ signal component, the dashed green line is for the remaining processes described by a third-order polynomial function, and the blue line is the total fit result.

The resulting χ_{6C}^2 is required to be less than 40. To reconstruct the η candidate, a seven-constraint (7C) kinematic fit is performed to further constrain the invariant mass of two photons to the m_{η} . Among the three $\gamma\gamma$ combinations, the one with the smallest χ_{7C}^2 is chosen. To suppress multi-photon backgrounds, the χ_{4C}^2 from the kinematic fit under the $J/\psi \rightarrow 7\gamma$ hypothesis is required to be less than that from the kinematic fits under the $J/\psi \rightarrow 8\gamma$ and $J/\psi \rightarrow 9\gamma$ hypotheses. The two photons from the η candidate are required to satisfy $|M_{\gamma\gamma} - m_{\eta}| < 27$ MeV/ c^2 . To suppress the miscombination between the radiative photon and other selected photons, events satisfying any of the following requirements are rejected: $|M_{\gamma_{\text{rad}}\gamma_{\pi^0}} - m_{\pi^0}| < 20$ MeV/ c^2 , $|M_{\gamma_{\text{rad}}\gamma_{\eta}} - m_{\pi^0}| < 20$ MeV/ c^2 , $|M_{\gamma_{\text{rad}}\gamma_{\pi^0}} - m_{\eta}| < 30$ MeV/ c^2 , and $|M_{\gamma_{\text{rad}}\gamma_{\eta}} - m_{\eta}| < 50$ MeV/ c^2 , where γ_{η} denotes the photons from the η candidate. With these requirements, the miscombination rate between the seven photons is 1.4%. To suppress background containing an ω , events with $|M_{\gamma_{\text{rad}}\pi^0} - m_{\omega}| < 40$ MeV/ c^2 are rejected. After applying the above selection criteria, clear $X(2370)$ and η_c peaks are observed in the $\pi^0\pi^0\eta$ invariant mass spectrum using the momenta obtained from the 7C kinematic fit, as shown in Fig. 3(a), Fig. 3(b), and Fig. 3(c). These two-dimensional distributions also indicate several possible intermediate processes, such as $f_0(1500)\eta$ and $a_0(980)^0 \pi^0 \rightarrow \pi^0\pi^0\eta$.

After applying the above selection criteria, no peaking

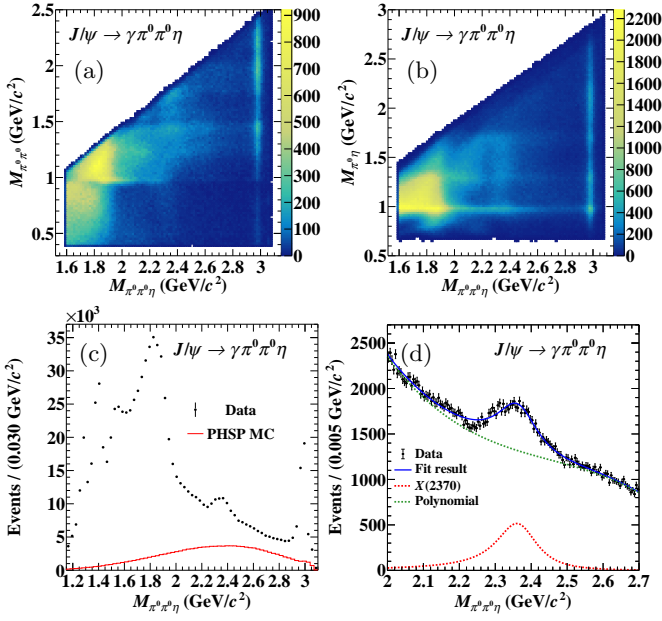


FIG. 3. The two-dimensional distributions of (a) $M_{\pi^0\pi^0}$ versus $M_{\pi^0\pi^0\eta}$ and (b) $M_{\pi^0\eta}$ versus $M_{\pi^0\pi^0\eta}$. (c) The $\pi^0\pi^0\eta$ invariant mass spectrum. The solid red histogram is from PHSP MC with arbitrary normalization. (d) The fit results within the range [2.00, 2.70] GeV/c^2 . The dashed red line is the $X(2370)$ signal component, the dashed green line is for the remaining processes described by a third-order polynomial function, and the blue line is the total fit result.

background is found in the $\pi^0\pi^0\eta$ invariant mass spectrum of the inclusive MC sample. The background contribution from non- η processes is estimated by fitting the corresponding $M_{\gamma\gamma}$ distribution in the data, yielding a non- η background fraction of 3.5%. A validation using η mass sideband events indicates that the non- η background processes produce no peaking structure. Therefore, it is described by a polynomial function in the subsequent fit.

A strategy analogous to that described for the $J/\psi \rightarrow \gamma K_S^0 K_S^0 \pi^0$ process is employed in the fit to the $\pi^0\pi^0\eta$ invariant mass spectrum between 2.0 and 2.7 GeV/c^2 , as shown in Fig. 3(d). The mass and width of the $X(2370)$ are measured to be $2366 \pm 2(\text{stat}) \text{ MeV}/c^2$ and $127 \pm 9(\text{stat}) \text{ MeV}$, respectively. The significance of the $X(2370)$ is greater than 20σ including systematic variations.

Based on the selection criteria for the $J/\psi \rightarrow \gamma\pi^0\pi^0\eta$ process described above, an $a_0(980)^0$ candidate is reconstructed from the η and the lower energy π^0 . To suppress the contribution from the decay $X(2370) \rightarrow f_0(1500)\eta$, events with $|M_{\pi^0\pi^0} - 1.5 \text{ GeV}/c^2| < 0.15 \text{ GeV}/c^2$ are rejected. The resulting mass spectrum of the η and the lower energy π^0 is shown in Fig. 4(a). An additional requirement of $|M_{\pi^0\eta} - 0.98 \text{ GeV}/c^2| < 0.05 \text{ GeV}/c^2$ is applied to select the $a_0(980)^0$ signal region. After applying these requirements, the $\pi^0\pi^0\eta$ mass spectrum, shown in Fig. 4(b), shows clear $X(2370)$ and η_c peaks. The $\pi^0\pi^0\eta$ mass spectrum between 2.00 and 2.70 GeV/c^2 is

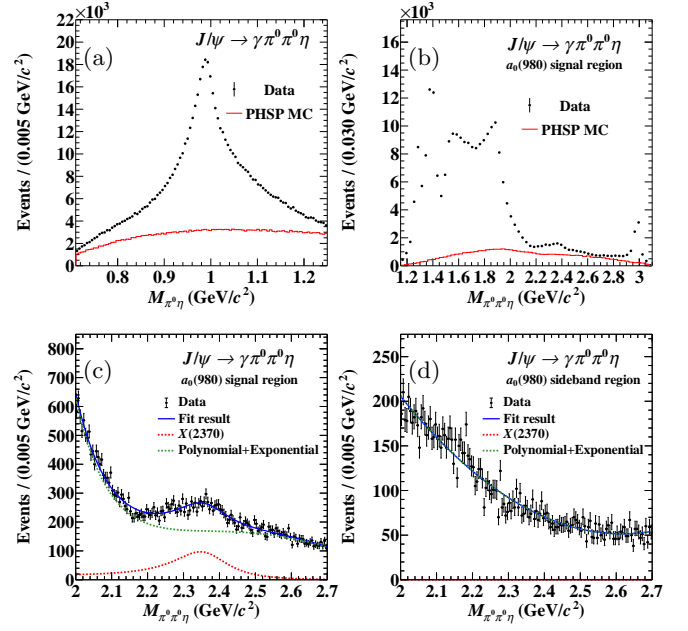


FIG. 4. (a) The invariant mass spectrum of the η and the π^0 with lower energy. (b) The $\pi^0\pi^0\eta$ invariant mass spectrum for selected events in the $a_0(980)$ signal region. The PHSP MC simulations are shown with arbitrary normalization. (c) and (d) are the fit results within the range [2.00, 2.70] GeV/c^2 for the $a_0(980)$ signal region and the $a_0(980)$ sideband region, respectively. The dashed green line is the contribution of the remaining processes described by the sum of a second-order polynomial and an exponential function.

fitted using a strategy analogous to that described in the last paragraph, as shown in Fig. 4(c). In particular, the PHSP in this fit includes an intermediate $a_0(980)^0$ state, which is parametrized using dispersion integrals [34]. The remaining processes are described by the sum of a polynomial and an exponential function. The mass and width of the $X(2370)$ are measured to be $2358 \pm 5(\text{stat}) \text{ MeV}/c^2$ and $180 \pm 20(\text{stat}) \text{ MeV}$, respectively. The significance of the $X(2370)$ is greater than 9σ including systematic variations. In contrast, there is no evidence of the $X(2370)$ signal in the $a_0(980)^0$ mass sideband region of $0.20 \text{ GeV}/c^2 < |M_{\pi^0\eta} - 0.98 \text{ GeV}/c^2| < 0.25 \text{ GeV}/c^2$, as shown in Fig. 4(d).

Systematic uncertainties associated with the invariant mass spectrum fits are evaluated for the three decay modes and primarily arise from the PHSP parametrization, the background model, and an additional resonance. For each source, alternative fits are performed and the largest deviations of the fitted mass and width of the $X(2370)$ from the nominal fit are taken as the corresponding systematic uncertainties. The uncertainty associated with the PHSP parametrization is studied by including an additional Blatt-Weisskopf barrier factor and PHSP variations among different intermediate resonances. For the $K_S^0 K_S^0 \pi^0$ mode, the alternative intermediate resonances $K_0^*(1430)$ and $a_0(980)^0$ are considered. For the $\pi^0\pi^0\eta$ mode, the alternative intermediate resonances $a_0(980)^0$ and $f_0(1500)$ are considered.

TABLE I. Systematic uncertainties on the mass (in MeV/c^2), width (in MeV) and significance (in σ) of the $X(2370)$ in different processes, denoted as ΔM , $\Delta\Gamma$, and N_σ , respectively.

Source	$J/\psi \rightarrow \gamma K_S^0 K_S^0 \pi^0$			$J/\psi \rightarrow \gamma \pi^0 \pi^0 \eta$			$J/\psi \rightarrow \gamma \pi^0 \pi^0 \eta$ ($a_0(980)^0$ signal region)		
	ΔM	$\Delta\Gamma$	N_σ	ΔM	$\Delta\Gamma$	N_σ	ΔM	$\Delta\Gamma$	N_σ
PHSP parametrization	± 7	± 2	> 18	± 3	± 1	> 20	± 2	± 3	> 12
Background model	± 10	± 37	> 14	± 9	± 24	> 20	± 9	± 58	> 9
Additional resonance	± 22	± 62	> 14	± 4	± 56	> 20	—	—	—
Total	± 25	± 72	> 14	± 10	± 61	> 20	± 9	± 58	> 9

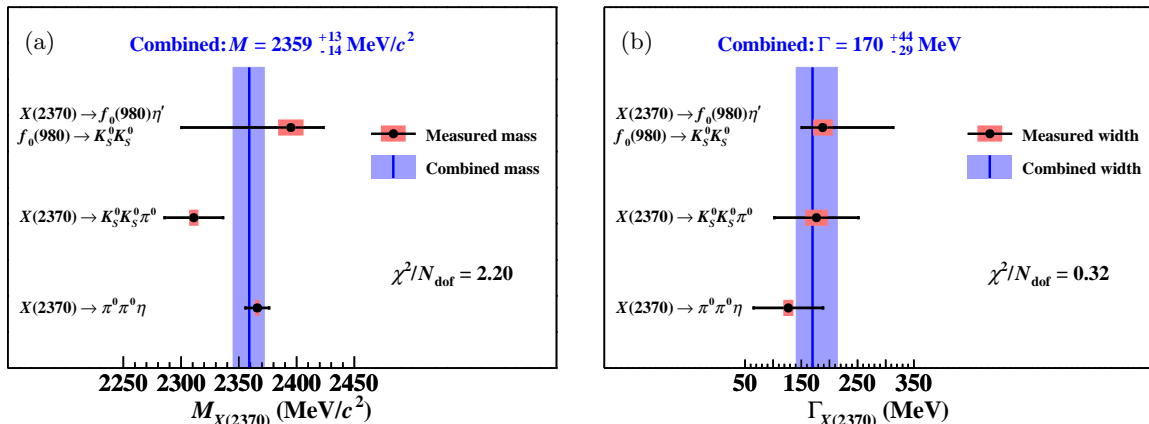


FIG. 5. Combined (a) mass and (b) width of the $X(2370)$. The bar on each black dot corresponds to the total uncertainty; the horizontal red shaded bands represent the statistical uncertainties; the vertical blue lines and blue shaded bands represent the combined results with total uncertainties.

The $a_0(980)^0$ is described using both the Flatté [34, 35] and dispersion-integral parametrizations [34], while all the other intermediate resonances are described by BW functions with masses and widths fixed to the PDG values [22]. The uncertainty related to the background model is estimated by varying the fit range and adopting alternative background parametrizations. The uncertainty related to an additional resonance is estimated by varying the treatment of the additional resonance. For the $K_S^0 K_S^0 \pi^0$ mode, the uncertainty includes a contribution from the additional resonance $X(2260)$. This inclusion is motivated by the study of the charged channel $J/\psi \rightarrow \gamma K_S^0 K^\pm \pi^\mp$ [36], where the $X(2260)$ is observed in the $K_S^0 K^\pm \pi^\mp$ mass spectrum with a significance greater than 10σ , and its fitted mass and width are $2256 \pm 3(\text{stat}) \text{ MeV}/c^2$ and $74 \pm 10(\text{stat}) \text{ MeV}$, respectively. The significance of the $X(2260)$ in the $K_S^0 K_S^0 \pi^0$

mass spectrum is 2.3σ , where the small significance is due to the statistics being more than ten times smaller here than in the charged channel. The uncertainty related to the impact of the $X(2260)$ is estimated by incorporating its contribution to the $K_S^0 K_S^0 \pi^0$ mass spectrum fit, and the mass and width of the $X(2260)$ are fixed to the values measured in the $K_S^0 K^\pm \pi^\mp$ mass spectrum. For the $\pi^0 \pi^0 \eta$ mode, a potential additional resonance can be added in the mass spectrum fit with a statistical significance of 4σ , and its mass and width are fitted to be $2142 \pm 7(\text{stat}) \text{ MeV}/c^2$ and $186 \pm 48(\text{stat}) \text{ MeV}$, respectively. The uncertainty related to the impact of this resonance is estimated by incorporating its contribution to the $\pi^0 \pi^0 \eta$ mass spectrum fit. For the $a_0(980)^0 \pi^0$ mode, since no evidence of the additional resonance is observed, the uncertainty related to the additional resonance is not included. All sources of systematic uncertainties are summarized in Table I.

To further improve the measurement precision, the $X(2370)$ masses and widths measured in different decay modes are combined following the procedure recommended by the PDG [22]. All of the $X(2370)$ measurements included in our combination are based on the data sample of 10 billion J/ψ events collected with the BESIII detector, including the studies of the $J/\psi \rightarrow \gamma K_S^0 K_S^0 \pi^0$ and $J/\psi \rightarrow \gamma \pi^0 \pi^0 \eta$ processes presented in this paper,

as well as the previously reported results in the $J/\psi \rightarrow \gamma K_S^0 K_S^0 \eta'$ process [12]. Considering the statistical and systematic uncertainties, the combined mass and width of the $X(2370)$ are $2359^{+13}_{-14} \text{ MeV}/c^2$ and $170^{+44}_{-29} \text{ MeV}$, respectively. The uncertainty of the combined mass is scaled by a factor of 1.48 due to $\chi^2/N_{\text{dof}} = 2.20$, following the procedure recommended by the PDG [22]. Figure 5 presents the comparisons of the $X(2370)$ resonance pa-

parameters measured in individual channels and combined as discussed in this paper. The resulting χ^2/N_{dof} values, shown on each figure and defined in the PDG [22], indicate reasonable consistency among input measurements.

In summary, using a sample of $(10087 \pm 44) \times 10^6$ J/ψ events [23] collected with the BESIII detector, the $J/\psi \rightarrow \gamma K_S^0 K_S^0 \pi^0$ and $J/\psi \rightarrow \gamma \pi^0 \pi^0 \eta$ processes are investigated to search for the $X(2370)$. The $X(2370)$ is observed in the $K_S^0 K_S^0 \pi^0$ and $\pi^0 \pi^0 \eta$ invariant mass spectra with statistical significances greater than 14σ and 20σ , respectively. By further selecting the $a_0(980)^0$ mass region in the latter process, the decay $X(2370) \rightarrow a_0(980)^0 \pi^0$ with $a_0(980)^0 \rightarrow \pi^0 \eta$ is observed with a statistical significance greater than 9σ . In the above decay modes, the mass and width of the $X(2370)$ are determined to be

$$1) X(2370) \rightarrow K_S^0 K_S^0 \pi^0 :$$

$$M_{X(2370)} = 2311 \pm 4(\text{stat}) \pm 25(\text{syst}) \text{ MeV}/c^2 ,$$

$$\Gamma_{X(2370)} = 177 \pm 20(\text{stat}) \pm 72(\text{syst}) \text{ MeV} ;$$

$$2) X(2370) \rightarrow \pi^0 \pi^0 \eta :$$

$$M_{X(2370)} = 2366 \pm 2(\text{stat}) \pm 10(\text{syst}) \text{ MeV}/c^2 ,$$

$$\Gamma_{X(2370)} = 127 \pm 9(\text{stat}) \pm 61(\text{syst}) \text{ MeV} ;$$

$$3) X(2370) \rightarrow a_0(980)^0 \pi^0 :$$

$$M_{X(2370)} = 2358 \pm 5(\text{stat}) \pm 9(\text{syst}) \text{ MeV}/c^2 ,$$

$$\Gamma_{X(2370)} = 180 \pm 20(\text{stat}) \pm 58(\text{syst}) \text{ MeV} .$$

Based on the results in the first two decay modes observed in this paper, together with the previously reported results in $J/\psi \rightarrow \gamma K_S^0 K_S^0 \eta'$ [12], a combination of the $X(2370)$ mass and width is performed, yielding

$$M_{X(2370)} = 2359_{-14}^{+13} \text{ MeV}/c^2 ,$$

$$\Gamma_{X(2370)} = 170_{-29}^{+44} \text{ MeV} .$$

The combined mass of the $X(2370)$ is within the mass range predicted by LQCD calculations for the lightest pseudoscalar glueball [5, 6]. The observed decay modes of $\pi^+ \pi^- \eta'$, $K_S^0 K_S^0 \eta'$, $K_S^0 K_S^0 \pi^0$, and $\pi^0 \pi^0 \eta$ including $a_0(980)^0 \pi^0$ show similarities between the $X(2370)$ and η_c decays. In addition, as shown in the scatter plot of $M_{K_S^0 K_S^0}$ versus $M_{K_S^0 K_S^0 \eta}$ from a previous study of the

$J/\psi \rightarrow \gamma K_S^0 K_S^0 \eta$ channel [37], similar behavior is observed in the $K_S^0 K_S^0 \eta$ decay mode. The numbers of events in both the $X(2370)$ and η_c mass region are enhanced in the $f_0(1500)$ and $f_0(1710)$ mass regions, while they are suppressed in the $f_0(980)$ mass region. The similarities in decay modes between the $X(2370)$ and η_c are consistent with the expected features of a pseudoscalar glueball. To further identify the nature of the $X(2370)$, more studies need to be performed both experimentally and theoretically.

The BESIII Collaboration thanks the staff of BEPCII (<https://cstr.cn/31109.02.BEPC>) and the IHEP computing center for their strong support. This work is supported in part by National Key R&D Program of China under Contracts Nos. 2023YFA1606000, 2023YFA1606704, 2025YFA1613900; National Natural Science Foundation of China (NSFC) under Contracts Nos. 11635010, 11935015, 11935016, 11935018, 12025502, 12035009, 12035013, 12061131003, 12192260, 12192261, 12192262, 12192263, 12192264, 12192265, 12221005, 12225509, 12235017, 12342502, 12361141819, 12535005; the Chinese Academy of Sciences (CAS) Large-Scale Scientific Facility Program; the Strategic Priority Research Program of Chinese Academy of Sciences under Contract No. XDA0480600; CAS under Contract No. YSBR-101; 100 Talents Program of CAS; The Institute of Nuclear and Particle Physics (INPAC) and Shanghai Key Laboratory for Particle Physics and Cosmology; Agencia Nacional de Investigación y Desarrollo de Chile (ANID), Chile under Contract No. ANID CCTVal CIA250027; ERC under Contract No. 758462; German Research Foundation DFG under Contract No. FOR5327; Istituto Nazionale di Fisica Nucleare, Italy; Knut and Alice Wallenberg Foundation under Contracts Nos. 2021.0174, 2021.0299, 2023.0315; Ministry of Development of Turkey under Contract No. DPT2006K-120470; National Research Foundation of Korea under Contract No. NRF-2022R1A2C1092335; National Science and Technology fund of Mongolia; Polish National Science Centre under Contract No. 2024/53/B/ST2/00975; STFC (United Kingdom); Swedish Research Council under Contract No. 2019.04595; U. S. Department of Energy under Contract No. DE-FG02-05ER41374.

[1] G. S. Bali, K. Schilling, A. Hulsebos, A. C. Irving, C. Michael, and P. W. Stephenson (UKQCD Collaboration), *Phys. Lett. B* **309**, 378 (1993).
[2] C. J. Morningstar and M. J. Peardon, *Phys. Rev. D* **60**, 034509 (1999).
[3] Y. Chen *et al.*, *Phys. Rev. D* **73**, 014516 (2006).
[4] E. Gregory, A. Irving, B. Lucini, C. McNeile, A. Rago, C. Richards, and E. Rinaldi, *JHEP* **10**, 170 (2012).
[5] L. C. Gui, J. M. Dong, Y. Chen, and Y. B. Yang, *Phys. Rev. D* **100**, 054511 (2019).
[6] D. Vadacchino, *PoS LATTICE2022*, 236 (2022),

[arXiv:2305.04869](https://arxiv.org/abs/2305.04869).

[7] L. Kopke and N. Wermes, *Phys. Rept.* **174**, 67 (1989).
[8] M. B. Çakır and G. R. Farrar, *Phys. Rev. D* **50**, 3268 (1994).
[9] F. E. Close, G. R. Farrar, and Z. Li, *Phys. Rev. D* **55**, 5749 (1997).
[10] M. Ablikim *et al.* (BESIII Collaboration), *Phys. Rev. Lett.* **106**, 072002 (2011).
[11] M. Ablikim *et al.* (BESIII Collaboration), *Eur. Phys. J. C* **80**, 746 (2020).
[12] M. Ablikim *et al.* (BESIII collaboration), *Phys. Rev.*

- Lett. **132**, 181901 (2024).
- [13] X. Sun, L. Y. Dai, S. Q. Kuang, W. Qin, and A. P. Szczepaniak, *Phys. Rev. D* **105**, 034010 (2022).
- [14] J. S. Yu, Z. F. Sun, X. Liu, and Q. Zhao, *Phys. Rev. D* **83**, 114007 (2011), arXiv:1104.3064 [hep-ph].
- [15] R. R. Dong, N. Su, H. X. Chen, E. L. Cui, and Z. Y. Zhou, *Eur. Phys. J. C* **80**, 749 (2020), arXiv:2003.07670 [hep-ph].
- [16] Q. N. Wang, D. K. Lian, and W. Chen, *Phys. Rev. D* **112**, 034010 (2025), arXiv:2502.16047 [hep-ph].
- [17] N. Su and H. X. Chen, *Phys. Rev. D* **106**, 014023 (2022), arXiv:2204.13959 [hep-ph].
- [18] K. T. Chao, *Commun. Theor. Phys.* **24**, 373 (1995).
- [19] T. Huang, S. Jin, D. H. Zhang, and K. T. Chao, *Phys. Lett. B* **380**, 189 (1996).
- [20] Y. Huang, S. Jin, and P. Zhang, *Int. J. Mod. Phys. A* **40**, 2530007 (2025).
- [21] C. Morningstar, *PoS LATTICE2024*, 004 (2024).
- [22] S. Navas *et al.* (Particle Data Group), *Phys. Rev. D* **110**, 030001 (2024).
- [23] M. Ablikim *et al.* (BESIII Collaboration), *Chin. Phys. C* **46**, 074001 (2022).
- [24] M. Ablikim *et al.* (BESIII Collaboration), *Nucl. Instrum. Meth. A* **614**, 345 (2010).
- [25] S. Agostinelli *et al.*, *Nucl. Instrum. Methods Phys. Res., Sect. A* **506**, 250 (2003).
- [26] K. X. Huang *et al.*, *Nucl. Sci. Tech.* **33**, 142 (2022).
- [27] S. Jadach, B. F. L. Ward, and Z. Wař, *Phys. Rev. D* **63**, 113009 (2001).
- [28] S. Jadach, B. F. L. Ward, and Z. Wař, *Comput Phys Commun* **130**, 260 (2000).
- [29] D. J. Lange, *Nucl. Instrum. Methods Phys. Res., Sect. A* **462**, 152 (2001).
- [30] R. G. Ping, *Chin. Phys. C* **32**, 599 (2008).
- [31] J. C. Chen, G. S. Huang, X. R. Qi, D. H. Zhang, and Y. S. Zhu, *Phys. Rev. D* **62**, 034003 (2000).
- [32] R. L. Yang, R. G. Ping, and H. Chen, *Chin. Phys. Lett.* **31**, 061301 (2014).
- [33] E. Barberio and Z. Was, *Comput. Phys. Commun.* **79**, 291 (1994).
- [34] M. Ablikim *et al.* (BESIII Collaboration), *Phys. Rev. D* **95**, 032002 (2017).
- [35] S. M. Flatte, *Phys. Lett. B* **63**, 224 (1976).
- [36] M. Ablikim *et al.* (BESIII Collaboration), *Observation of the X(2370) in $J/\psi \rightarrow \gamma K_S^0 K^\pm \pi^\mp$* , publication in preparation.
- [37] M. Ablikim *et al.* (BESIII Collaboration), *Phys. Rev. Lett.* **115**, 091803 (2015).